HYDRODYNAMIC PARAMETER ESTIMATION OF AN UNMANNED UNDERWATER VEHICLE

Juan Julca Avila
juan.avila@poli.usp.br

Jorge Julca Avila
jorge.avila@poli.usp.br

Newton Maruyama
maruyama@usp.br

Julio Cezar Adamowski
jcadamow@usp.br

Departamento de Engenharia Mecatrônica, Escola Politécnica da Universidade de São Paulo, Av. Prof. Mello Moraes, 2231, CEP 05508-900, São Paulo, SP

Abstract. *A semi-autonomous Underwater Unmanned Vehicle testbed is being developed at the Escola Politécnica at the University of São Paulo in order to provide inspection and intervention capabilities for missions in deep water oil fields. The vehicle is named Underwater Robotic System. With the aim of predicting the maximal velocity that an unmanned underwater vehicle may reach during its translation movement, under maximum thruster power condition, hydrodynamic parameters must be estimated. In this work, an experimental approach to estimate hydrodynamic parameters in surge, sway and heave motions is introduced. Two sets of tests are performed. In the first set, drag coefficients are estimated with the vehicle under constant velocity in a towing tank. In the second set, a mass-spring assembly is used to estimate added mass coefficients of the vehicle. The experimental setup is a cage structure which holds the reduced scale model using a set of eight springs allowing free vertical oscillation motions. The natural frequency of vibration is measured with ac accelerometer during a free oscillating motion. An additional experimental setup is performed for thruster parameter estimation. With hydrodynamic coefficients in hand, together with thruster parameters, the maximal velocities in* surge, sway *and* heave *are predicted. In order to compare with experimental results drag coefficients estimates are also obtained numerically using the CFD FLUENT software, giving some support for validation of our experimental results.*

Keywords: *Unmanned underwater vehicle, hydrodynamic parameter estimation, towing tank CFD-Computational Fluid Dynamics*

1. Introduction

A semi-autonomous Underwater Unmanned Vehicle (UUV) testbed is being developed at the Escola Politécnica at the University of São Paulo in order to provide inspection and intervention capabilities for missions in deep water oil fields. The vehicle is named Underwater Robotic System (URS). The semi-autonomous characteristic of the URS is related with the presence of a tether cable for information carrying and also vehicle positioning and recovery, however, the vehicle behaves autonomously when close to the target. One must think of the URS as having characteristics of a Remotely Operated Vehicle (ROV) and an Autonomous Underwater Vehicle (AUV). The first devised mission is related to transponder recovery. Dynamic positioning of the vehicle will be executed through a precise acoustic navigation system together with embedded control and propulsion systems. The vehicle aimed to this mission is an open-frame type that includes pressure vessels for instrumentation and control, and a set of eight undersea thrusters.

In recent years, there have been intensive efforts towards the development of unmanned underwater vehicles, see for example (Wernli, 2002) for an AUV technology survey. In order to design an UUV, its maneuverability and controllability must be examined in advance, preferably based on a mathematical model. The mathematical model contains hydrodynamic forces and moments expressed in terms of a set of hydrodynamic coefficients. Therefore, it is important to know the true value of these coefficients to simulate the performance of UUVs accurately.

Hydrodynamic coefficients may be classified into three types: linear damping coefficients, linear inertial force coefficients, and nonlinear damping coefficients. Among these, the linear damping coefficients mostly affect the maneuverability of an UUV (Kim et. al., 2002). These coefficients might be estimated using experimental setup, numerical analysis or empirical formula. The usual parameter estimation procedure involves long and expensive tank testing on a Planar Motion Mechanism (PMM). Following trials, considerable effort is needed to derive a mathematical model from experimental results, leading to a prohibitively expensive model which will be inaccurate as soon as hydrodynamic characteristics are altered, for example by adding an auxiliary equipment.

With the aim of predicting the maximal velocity that an unmanned underwater vehicle, under maximum thruster power condition, may reach during translation movements, hydrodynamic parameters must be estimated. In this work, an experimental approach to estimate hydrodynamic parameters in em surge, *sway* and *heave* motions is introduced. Only hydrodynamic parameters of the vehicle itself are considered, leaving behind the tether cable dynamics.

Two sets of experiments have been performed. In the first set, drag coefficients are estimated with the vehicle under constant velocity in a towing tank. In the second set, a mass-spring assembly is used to estimate added mass coefficients. The experimental setup is a cage structure which holds a reduced scale model using a set of eight springs allowing free vertical oscillation motions. The natural frequency of vibration is measured with an accelerometer during a free oscillating motion. Using the natural frequency information the added mass can be calculated. An additional experimental setup is performed for thruster parameter estimation. With the hydrodynamic coefficients in hand, together with thruster parameters, the maximal velocities in *surge*, *sway* and *heave* are predicted. In order to compare with experimental results drag coefficients estimates are also obtained numerically using the CFD FLUENT software, giving some support for validation of our experimental results

The paper is organized as follows. In Section 2, the adopted simplified dynamic model of the URS is presented. In Section 3, a brief overview of the URS mechanical design is introduced. The experimental approaches for the drag and added mass hydrodynamic coefficients are reported in Section 4. Section 5 presents the thruster static model and the experimental setup designed for parameter identification. Also, after all hydrodynamic parameters and thruster parameters are known some simulations are performed to predict the maximal velocity in all motion directions. Section 6 presents the numerical drag coefficients which are estimated with the CFD program FLUENT. Finally, in Section 7 some concluding remarks are drawn.

2. The reduced URS dynamic model

The URS dynamic model can be derived from the general Newton-Euler motion equations of a rigid body in a fluid medium. If the fluid is irrotational, inviscid, of uniform and constant density, and of infinite extent, then the motion equations in its six DOFs can be written in a local reference frame (Indiveri, 1998). The dynamic equations of an UUV are composed by a group of six non linear differential equations of second order. These equations are coupled and with large number of coefficients, which makes their utilization for parameter estimation very complex. Depending on the number of symmetry plans, the localization of the center of coordinates, and the absolute velocity value, these equations might be simplified. In the case of the URS, the vehicle design has been specified to be intrinsically stable in both *roll* and *pitch* and the nominal absolute velocity value is adopted as 1.0m/s. In this context, a decoupled dynamic model may be written for the estimation of the drag and added mass hydrodynamic coefficients. When considering a pure translation motion together with the hypothesis that the total hydrodynamic force is mostly due to drag and added mass components and also that the thruster force τ in this direction is known, the following mathematical model, that has been used for the vehicle design, may be written (Sarpkaya and Isaacson, 1981; Marco et. al., 1998):

$$\eta\tau = \frac{1}{2}C_D\rho A_c|U|U + (m + m_{ad})\frac{dU}{dt}, \tag{1}$$

where A_c is the body characteristic area, C_D is the drag coefficient, ρ is the fluid density, m is the body mass e m_{ad} is the added mass. U is the vehicle translation velocity. The η coefficient represents a power loss factor in the propulsion system. the η coefficient assume values between 0 and 1, depending on thruster geometric distribution together with interactions vehicle/thruster and thruster/thruster.

3. Mechanical design

The mechanical structure of the URS is designed as an open frame vehicle. Attached to the stainless steel tubular framework there are eight thrusters and four stainless steel pressure vessels, where two of them, in the upper part, carry batteries and the remaining two, in the bottom part, carry the embedded electronics and sensors. Fig. 1(a) illustrates the mechanical structure of the URS which has $1278mm$, $1114mm$ and $800mm$ respectively for length, depth and height dimensions. The total mass is approximately $420Kg$ with a displaced volume of $0.189m^3$. In the bottom part, there are four thrusters which are used for vertical movements, and four thrusters, for horizontal movements, are disposed right above the midway horizontal plane section. Fig. 1(b) illustrates the URS reduced scale model (1:2) which has undertook experimental trials in a towing tank.

Table 1. Model drag coefficient in the *surge* direction C_{D_x}.

Velocity (m/s)	$F_D(N)$	Reynolds Number R_e	Drag coefficient C_{D_x}
0.2	3.846 ± 0.137	0.568×10^5	2.336 ± 0.083
0.3	8.721 ± 0.255	0.852×10^5	2.355 ± 0.069
0.4	14.077 ± 0.235	1.135×10^5	2.138 ± 0.036
0.5	23.289 ± 0.343	1.419×10^5	2.264 ± 0.033
0.6	33.236 ± 0.442	1.703×10^5	2.243 ± 0.030
0.7	45.126 ± 0.471	1.987×10^5	2.238 ± 0.023
0.8	57.967 ± 0.549	2.271×10^5	2.201 ± 0.021

4. Hydrodynamic parameter estimation

4.1 Drag coefficients

Some experimental trials are performed with constant velocity in a towing tank in order to obtain the dependence of the drag coefficient with the Reynolds number. The dimensionless parameters:

$$R_e = \frac{U\forall^{1/3}}{\nu} \quad \text{Reynolds number,}$$
$$C_D = \frac{F_D}{\frac{1}{2}\rho U^2 \forall^{2/3}} \quad \text{Drag coefficient,}$$

are defined depending on the volume of fluid displaced by the vehicle $\forall$ (Nomoto and Hattori,1986). $\forall^{1/3}$ is the characteristic length and $\forall^{2/3}$ is the body characteristic area. The water viscosity is $\nu = 1.01 \times 10^{-6} m^2/s$ and the displaced volumes are: $\forall_m = 0.0236 m^3$ (model) and $\forall_t = 0.1885 m^3$ (testbed).

4.1.1 Experimental approach

In this experiment, the reduced scale model is hold by a mobile car. The car moves on rail while pushing the scale model in a constant velocity (See Fig. 2). The drag coefficient can be estimated using the measured torque in a load cell. A drag force F_D is originated when the car/bar/model set moves through the tank with constant velocity U. The drag force F_D is transferred to the load cell through an articulated bar. Using the force measured by the load cell F_{cel}, the drag force F_D can be estimated using the Archimedet's lever law. The force F_D is then calculated according to:

$$F_D = \frac{l_1}{l_2} F_{cel}, \tag{2}$$

where l_1 and l_2 are the lengths of the two parts of the bar which are defined by the fulcrum. The length l_2 depends on the pressure center. The pressure center can be approximated by the geometric center of the zy plane. The pressure center of the model are calculated with AUTOCAD, $123.6mm$ in *surge* direction, $262.0mm$ in *sway* direction and $4288.0mm$ in *heave* direction.

In order to obtain the curves of the drag coefficients in *surge*, *sway* and *heave* motins, the car velocity is varied from $0.2m/s$ to $0.8m/s$ with increments of $0.1m/s$. Table 1 summarizes the results for drag force F_{D_x}, Reynolds number R_e, and drag coefficient C_{D_x} in the *surge* direction. We omit the experimental results for *sway* and *heave* motions due to space restrictions.

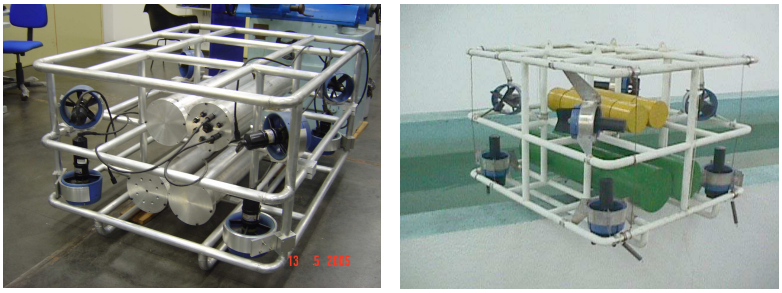

(a) The URS. (b) The model.

Figure 1. The Underwater Robotic System and the reduced scale model.

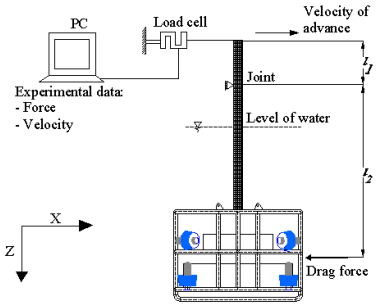

Figure 2. Experimental setup for drag coeficient estimation.

Table 2. Mean values for drag coefficients C_D.

surge	*sway*	*heave*
2.243 ± 0.03	2.728 ± 0.029	3.617 ± 0.029

The experimental results show that drag coefficients in *surge*, *sway* and *heave* are approximately constant for Reynolds number R_e above 1×10^5. Table 2 shows the mean values for drag coefficients in the considered motions.

4.2 Added mass

The added mass forces and moments derive from accelerations that fluid particles experience when they encounter a moving body structure. The added mass is defined as the hydrodynamic pressure induced force, which is proportional to the acceleration. In practice, this added mass acts as having being incorporated into the body structure mass (Newman, 1977). If a totally submerged body structure is accelerated from finite velocity, together with the drag force F_D another extra resistance force is incorporated. This extra force is modeled as being proportional to the vehicle acceleration, with the added mass m_{ad} being the proportional constant.

4.2.1 Experimental approach

An estimation of added mass of fully submerged structures can be obtained by carrying out free oscillation tests. The experimental setup is a cage structure which holds the scale model using a set of eight springs (See Fig. 3(a)). The free oscillation test is performed by releasing the model from an initial displaced position. In this way, the model realizes free oscillation movements like a mass-spring system. The natural frequency f_n can then be determined and consequently the added mass m_{ad}.

The estimates for the natural frequency of oscillation f_n can be calculated by (Sarpkaya and Isaacson, 1981):

$$f_n = \frac{1}{2\pi}\sqrt{\frac{k_{eq}}{m + m_{ad}}}, \tag{3}$$

where f_n is the model natural frequency; m is the effective model mass in air; m_{ad} is the added mass and k_{eq} is the effective spring constant when in water. Assuming that, for small displacements, the spring constant value is the same when immersed in either air or water, together with estimates for the natural frequency f_n, the added mass m_{ad} can be estimated using Eq. 3. The natural frequency values f_n are estimated using measurements of a piezoelectric accelerometer

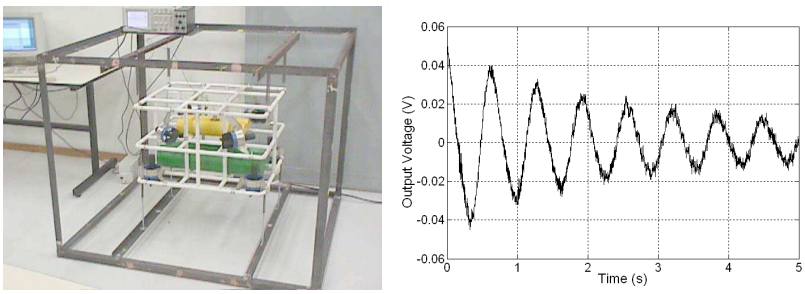

(a) (b)

Figure 3. (a) The experimental setup for added mass estimation. (b) Accelerometer measured signals when oscillating in the *sway* direction.

Table 3. Model added mass m_{ad} estimates.

	surge	*sway*	*heave*
$f_n(Hz)$	1.771	1.648	1.404
$m_{ad}(Kg)$	9.645 ± 0.243	14.855 ± 0.280	29.533 ± 0.386

Table 4. URS added mass $m_{ad}(Kg)$ estimates.

surge	*sway*	*heave*
81.81 ± 2.05	12.6 ± 2.38	250.71 ± 3.28

which is located in one of the model symmetry planes.

Fig. 1(b) illustrates accelerometer measurement signals when the model is oscillating in the *sway* direction. Table 3 illustrates the experimental results in the considered motions. The natural frequency f_n in the ***heave*** motion is smaller when compared to the values in other motions. This is due to, when in *heave* direction the motion is perpendicular to the pressure vessels, resulting in a larger hydrodynamic resistance area.

In order for free oscillation tests be useful there must be no flow separation. The condition for the non occurrence of flow separation can be reached if both maximum signal amplitude A and the natural frequency f_n are relatively small. This can be achieved by choosing appropriate springs. Assuming that, the model mass value is $m = 240Kg$, the effective spring constant value is $k_{eq} = 4585.8N/m$, then the natural frequency estimate value is $f_n = 2.2Hz$ in air.

The added mass m_{ad} is a measure of fluid inertia and not of viscous effects. In the free oscillation tests, one must ensure that the drag force F_d is not significant when compared to the added mass force F_{ad}, i.e., that the viscous effects might be omitted. This is supported by the following experimental observations (See Fig. 3(b)): a) the vertical oscillation velocity has sinusoidal shape, b) the damping is relatively small (Stelson and Mavis, 1955). One possible estimate for the relation between the added mass force F_{ad} and the drag force F_d is given by the Keulegan-Carpenter number:

$$KC = \frac{2\pi A}{D}, \tag{4}$$

where A is the maximum amplitude oscillation and D is the characteristic length. For the *surge* direction case, where $A = 50mm$ is the maximum amplitude signal and $D = 121mm$ is the correspondent cylinder diameter of the reduced model pressure vessel, then $KC = 2.6$. Sarpkaya and Isaacson (1981), state that for KC smaller than 10 the added mass forces are more significant than drag forces. Based on this, our estimates of the added mass m_{ad} are validated. With the following equation:

$$\left(\frac{m_{ad}}{\forall_m}\right)_{model} = \left(\frac{m_{ad}}{\forall_t}\right)_{testbed}, \tag{5}$$

the added mass m_{ad} of the testbed can be estimated, as the model added mass $m_{ad} = 22.2Kg$, the displaced volumes of the model $\forall_m = 0.0222m^3$ and the displaced volume of the testbed $\forall_t = 0.1885m^3$ are all known. Table 4 presents the estimates for the added mass in all three motion directions.

5. Dynamic response of the URS

5.1 Thruster parameter identification

An experimental setup has been designed in a water tank in order to estimate the thruster characteristic operation curve. The experiments are performed in *bollard-pull* condition. Fig. 4(a) illustrates the schematic diagram of the experimental setup. The Archimede's lever law is used to calculated the thrust when a voltage is applied to the electrical DC motor. A load cell which is located in the upper part of the bar measures the momentum generated in relation to the fulcrum.

According to Fig. 4(b), the thrust, in stationary conditions, is a quadratic function of the applied voltage. The following model is considered:

$$\tau = cV|V|, \tag{6}$$

where c is the thrust constant and V is the applied voltage. For the tested thruster, the constant $c = 9.423 \pm 0.0807N/V^2$ is for positive voltage values and $c = 6.551 \pm 0.0579N/V^2$ for negative voltage values.

5.2 Maximal velocity estimation of the URS

The dynamic response of the URS subject to a step input might be obtained using Eq. 1 in Table 5, we summarize the estimates of the coefficient values related to Eq. 1. Together with, the testbed body mass $m = 420Kg$, testbed

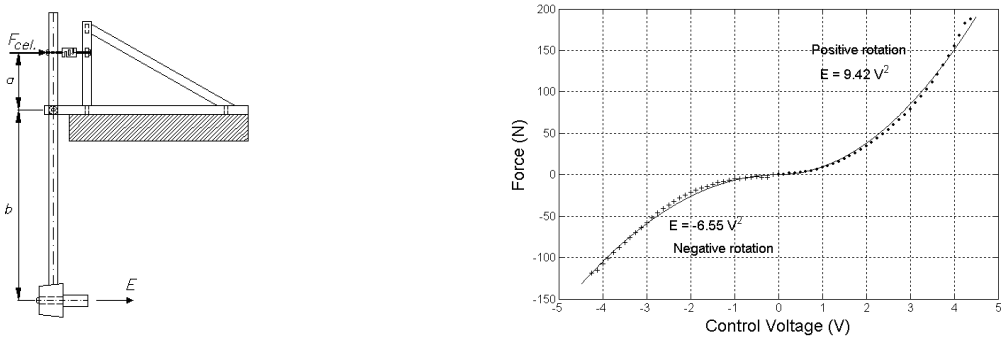

(a) (b)

Figure 4. (a) Experimental setup for thruster identification. (b) Thruster characteristic operation curve.

Table 5. Simulation parameters an maximal velocity estimation.

dof	C_D	$m_{ad}(Kg)$	$\tau(N)$	η	*max. vel. (m/s)*
surge	2.24	81.81	497.8	0.75	1.01
sway	2.73	126.11	348.6	0.75	0.76
heave	3.62	250.71	772.0	1.00	1.14

characteristic area $A_c = 0.329m^2$, and water density $\rho = 1000Kg/m^3$, it is possible to write down Eq. 1 for *surge*, *sway* and *heave* motions and calculate the maximal velocity that the vehicle can reach. Figure 5 illustrates the vehicle dynamic response for step input. The maximal velocity in each motion direction is reached in steady-state. Table 5 also summarizes the results for maximal velocity.

6. Numerical calculation of drag coefficients

In order to make comparisons with experimental results, drag coefficients have been estimated with the CFD program FLUENT 6. While considering one inlet velocity value, the fluid flow around the testbed is modeled with the continuity equation and the Navier-Stokes for incompressible fluid flow. The variables that need to be estimated are fluid velocity and pressure. The fluid domain environment is defined by the immersion of the testbed model in a parallelepipedus shaped water. The GAMBIT program has been utilized to establish an unstructured mesh which defines the fluid computational domain. The fluid computational domain has been discretized by 2057845 tetrahedral elements (See Fig. 6). A numerical solution for fluid velocities in the range of $0.2m/s$ to $0.8m/s$ with steps of $\Delta = 0.1m/s$. The average CPU time for each chosen velocity is 5h30min with 20 iterations in a Compaq Alpha Digital DS20E workstation.

6.1 Numerical results

For a constant velocity, the program determines the total hydrodynamic force and momentum acting on the vehicle. The adopted coordinated system is fixed in the center of gravity of the vehicle. The program decompose the forces/momentum into their corresponding orthogonal components. Here, we present only results related to the *surge* direction. Table 6 shows the numerical simulation results. One must note that when the vehicle is moving in the *surge* direction, the components related to *sway* and *heave* are not significant.

For the open frame type UUV the Reynolds number R_e is defined by the following expression

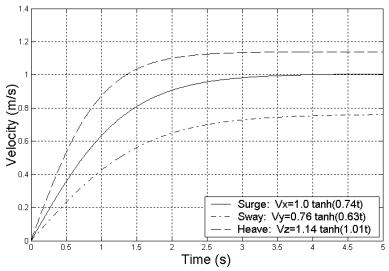

Figure 5. Step dynamic response of the URS in *surge*, *sway* and *heave* motions.

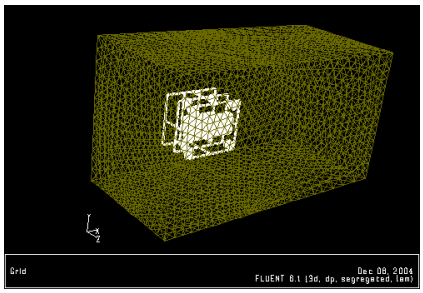

Figure 6. Computational domain.

Table 6. Numerical drag coefficient C_{D_x} and force F_{D_x} for the *surge* motion.

Vel. (m/s)	$F_{D_x}(N)$	$F_{D_y}(N)$	$F_{D_z}(N)$	R_e	C_{D_x}
0.2	4.187	0.0037	-0.0213	0.568×10^5	2.547
0.3	9.360	0.0097	-0.0514	0.852×10^5	2.531
0.4	16.578	0.0169	-0.0921	1.135×10^5	2.522
0.5	25.854	0.0298	-0.1465	1.419×10^5	2.517
0.6	37.120	0.0391	-0.2501	1.703×10^5	2.510
0.7	50.543	0.0430	-0.3019	1.987×10^5	2.510
0.8	64.760	0.0500	-0.4012	2.271×10^5	2.463

(Nomoto and Hattori, 1986):

$$R_e = \frac{U\forall^{1/3}}{\nu}, \tag{7}$$

where U represents the fluid flow velocity represents, $\forall = 0.02356m^3$ represents the displaced volume, and $\forall^{1/3}$ is the characteristic length. The water cinematic viscosity is $\nu = 1.01 \times 10^{-6}m^2/s$ (19^oC). Table 6 illustrates the drag coefficient C_{D_x} as a function of the Reynolds number R_e.

The following figures illustrates the flow velocity vector profiles. Fig. 7 shows the velocity vectors in a plane parallel to the plane defined by xz. Fig. 8 shows the velocity vectors in a parallel plane to the plane defined by xy.

According to Table 6 model drag coefficients in the *surge* movement direction are approximately constant for velocities between 0.2 and $0.8m/s$. Within this range of velocities the hydrodynamic quadratic law variation is verified and the flow is laminar. The boundary layer in the point of separation is laminar and the downstream wake is also laminar. According to Fig. 8, the presence of cylinder downstream vortex indicates that the flow can enter the critical phase with the increase of velocity above $1.0m/s$. If it gets into critical phase, analogous to flow around spheres, the downstream wake becomes turbulent and consequently the drag force diminishes.

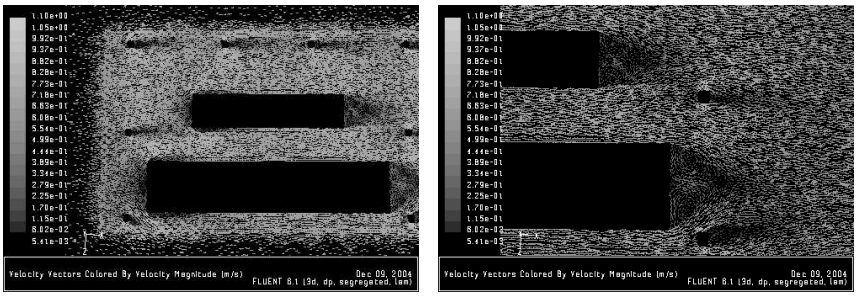

(a) Velocity vectors in one of the planes parallel to the xz plane.

(b) Downstream velocity vectors. Velocity $U = 0.7m/s$.

Figure 7. Velocity vectors in the xz plane.

6.2 Comparisons with experimental results

The numerical results for drag coefficients have been compared to the ones obtained experimentally by Avila (2003). Fig. 9 illustrates these comparisons. The experimental results are around 8% lower than the numerical results.

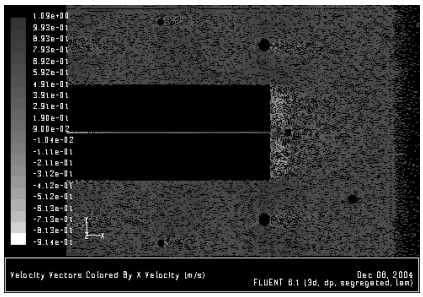

Figure 8. Velocity vectors in one of the xy planes.

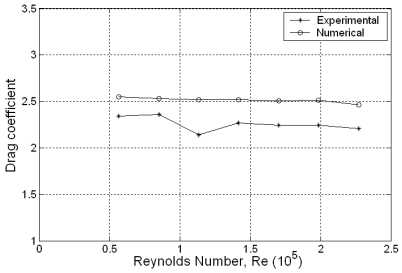

Figure 9. Comparisons between experimental and numerical results for the drag coefficients.

7. Conclusions

A maneuverability evaluation of an unmanned underwater vehicle is directly related to the knowledge of its hydrodynamic characteristics which can be translated by its hydrodynamic coefficients. In this paper, we have proposed an experimental approach, based on a reduced scale model, for estimation of the drag and added mass coefficients. The drag coefficients have been estimated using a towing tank approach. The added mass coefficients have been estimated using a mass-spring assembly. With the hydrodynamic coefficients in hand, together with thruster parameters, we have been able to predict the maximal velocities in *surge*, *sway* and *heave*. The drag coefficients estimates have been also obtained numerically and have come close to the experimental results, giving support for the validation of our approach. Added mass numerical calculation is under consideration for future work.

8. Acknowledgments

The authors would like to thank the FINEP who sponsored the project through the CTPetro Program; the CNPq, CAPES and FAPESP for the scholarship financial support and the CENPES-PETROBRAS for the logistic support.

9. References

Wernli, R. 2002. "AUVs - a technology whose time has come", IEEE International Conference in Underwater Tecnologies 2002.

Kim, J., Kim, K., and Choi, H., 2002. "Estimation of Hydrodynamic Coefficients for an AUV Using Nonlinear Observers", IEEE J. Oceanic Eng., Vol 27, No 4, pp 830-840.

Sarpkaya, T. and Isaacson, M., 1981. "Mechanics of Wave Forces on Offshore Structures", New York, Van Nostrand Reinhold.

Stelson, T.E., Mavis, F.T.. "Virtual mass and accelerations in fluids", 1955. Proc. ASCE, 81, p. 1-9.

Indiveri, G., 1998. "Modelling and identification of underwater robotic systems," Ph.D. dissertation, DIST Univ. of Genova, Italy.

Nomoto, M. and Hattori, M., 1986. "A deep ROV 'Dolphin 3K:' Design and performance analysis," IEEE J. Oceanic Eng., Vol 11, pp. 373-391.

Avila, J.J., 2003. "Estimação de coeficientes Hidrodinâmicos de um Veículo Submarino Semi-Autônomo", Dissertação de Mestrado, Escola Politécnica da Universidade de São Paulo.

Newman, J.N., 1977. "Marine Hydrodynamics". Cambridge, MA: MIT Press.

Marco, D.B., Martins, A., and A. J. Healey, J., 1998. "Surge motion parameter identification for the NPS Phoenix AUV" in IARP-1st Int. Workshop on Autonomous Underwater Vehicles for Shallow Water and Coastal Environment, Lafayette, pp. 197-210.